Installation and commissioning of a piezo-drive motor for a continuous G0-scan and parameter space optimisation for X-ray Dark-Field Radiographic (X-DFR) imaging

Bachelor Thesis

Leonie Sommer
sommerle@student.ethz.ch

May 31, 2021

Supervisor: Prof. Dr. Marco Stampanoni
Advisors: Dr. Michał Rawlik, Simon Spindler

Department of Information Technology and Electrical Engineering, ETH Zürich

Abstract

Because of the COVID-19 pandemic lung illnesses are a very current topic and are receiving a lot of attention. To recognise lung illnesses early cheap and fast imaging is very important. For this a Talbot-Lau interferometry setup is a promising option. To achieve the best possible image quality the Talbot-Lau interferometer was manually aligned. Additionally, different gratings were tested, and the best was used as G0. In this thesis a piezo motor to move the absorption grating G0 continuously was implemented. The phase-stepping and tomography measurement functions were written for both discrete and continuous movement. In comparison to the phase-stepping of G0 the improvement of the continuous movement in image quality has not been very noticeable. But the continuous movement offers future experiments with different movement patterns to improve acquisition time and quality.

Acknowledgement

I want to thank Professor Marco Stampanoni for the opportunity to participate in this interesting field as part of my bachelor thesis.
I would also like to thank my supervisors Dr. Michał Rawlik and Simon Spindler for the introduction to the setup, the extensive and interesting inside and the great support with my thesis.
Lastly, I would like to thank the GI-BCT team. It was a very inspiring time for me in which I gained a lot of knowledge.

Contents

Chapter 1

Introduction

Lung illnesses, for example chronic obstructive pulmonary disease (COPD), are very common and responsible for many casualities. Because of the COVID-19 pandemic, which can also affect the lung, this topic is currently getting more attention than in recent years. The diagnosis for COPD often happens very late in the progression of the illness. It is therefore of interest to provide a low-cost and fast possibility to check the lungs and detect illnesses early. X-ray imaging as a non-invasive procedure is already widely used in the medical field, for example to detect fractures in bones. It is almost always attenuation based. With x-ray grating interferometry can in addition to attenuation also refraction (differential phase contrast) and scattering (dark-field) be analysed. In attenuation based imaging of less absorbent materials, for example soft tissue, the contrast is very low where as the contrast in the refraction is higher. [2] Micro structures of the sample are better visible in dark-field imaging. [5] It shows that dark-field radiography looks very promising for imaging lungs cost-effective and fast.

1.1 Focus

The aim of this thesis is to incorporate a P-841.60 piezo-motor, which is used to move the source grating G0, into an existing Talbot-Lau interferometer setup. This entails the commissioning of the piezo-motor, the implementation of the controls compatible with the existing interface of the setup.
In order to obtain uniform intensity on the detector the Talbot-Lau interferometer was aligned. Furthermore, multiple gold plated graphite-gratings for G0 were compared to each other in terms of the visibility where the best one was chosen for all further measurements.
On the optimized setup, the continuous movement of G0 with the new piezo-motor was compared to the phase-stepping, in terms of visibility and practicality.

1.2   X-ray

X-rays are electromagnetic rays with a wavelength of 0.01nm to 10nm [3, p.120].

Absorption image   The concept of x-ray absorption imaging is based on the energy loss of the x-rays when they travel through matter. This energy loss is dependent on what kind of material the x-rays travel through. [3, p.120] For example, more x-rays are absorbed in bone than in soft tissue.

Medicine   Because of this, x-ray imaging is often used in medicine as a non-invasive procedure. The difference in absorption does make it possible to see the bone in an x-ray image, and for example, detect a fracture. [3, p.138] Absorption images work well for matter that absorbs a lot of the x-rays. To get the same contrast in the image for less absorbent materials, more x-rays are needed. [2] This dependence of dosage and contrast is one of the known limitations in the application of x-ray imaging in the medical field. Because x-ray are high energy rays they can ionize the materials they pass through. This can increase the risk to develop cancer. [3, p.122] Therefore a person should not be exposed to a high dosage of x-ray radiation.

X-ray imaging in the medical field almost exclusively utilizes the absorption of x-rays in material. A possible solution to avoid the required high dosage of x-rays for good contrast in images with low absorbing materials, is to implement x-ray grating interferometry.

Refraction   The interaction of x-rays with matter can be described through refraction in addition to absorption. The advantages of refraction based images are, that it may be possible to image materials with nearly identical absorption properties. [3, p.192] A setup which implements the principle of phase-contrast imaging is Talbot-Lau interferometry (see section 1.3).

1.3   X-ray grating interferometry

In comparison to medical x-ray imaging, which is mostly absorption based, in x-ray grating interferometry, phase and scattering can be analyzed. With the phase sensitivity, high contrast in imaging soft materials can be achieve. [2]

Talbot-Lau interferometry   For x-ray grating interferometry with a low coherence x-ray source, the Talbot-Lau interferometer setup is used. An example of the Talbot-Lau interferometer setup can be seen in figure 1.1. It consists of an X-ray source, three gratings (G0, G1 and G2) and a detector, lined up in the beam line. The sample can be positioned between G0 and
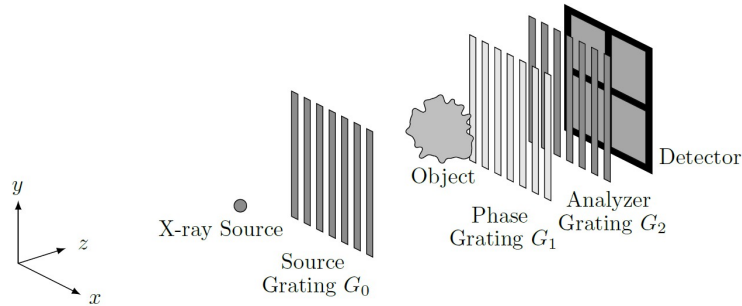
Figure 1.1: Talbot-Lau interferometer. Between X-ray source and detector three gratings G0, G1, G2, the form an interferometer. [3, p.195]

G1 (as seen in figure 1.1) or between G1 and G2 (as seen in figure 2.1). Each grating consists of slits and bars. The gratings G0 and G2 are absorption gratings and G1 is the phase grating. The purpose of G1 is to shift the wave coming through the grating by an additional factor. This phase shift only happens at the bars of the grating. The wave passes through the slits without any change. Because of this periodic phase modulation in certain wave sections, interference (destructive or constructive) between the wave sections can occur. [3, p.195] Figure 1.2 shows a simulation of the resulting interference pattern after G1. Because of the Talbot effect, the pattern repeats itself periodically. Therefore the detector (which has to be placed somewhere, where the interference pattern is observable as distinctly black and white) could be placed at each of those positions, which are periodically repeated. But because the interference pattern becomes less distinct over the course of multiple periods, the detector has to be placed within the first periods of the pattern. [3, p.196]

The grating G0 is positioned right after the x-ray source. For the interference patter to be visible, the x-ray source has to be spatially coherent. But because the x-ray tube has to be able to produce enough x-rays so that the imaging time is not too long, the focal spot is too big. Hence, the absorption grating G0 is positioned after the source. Each of the slits of this grating focuses the x-rays to a smaller spot. The distance between the slits has to be chosen in a way, so that the interference pattern of the slits after G0 exactly overlay with each other. This produces a spatially coherent x-ray beam after G0. [3, p.196]

The grating G2 in front of the detector is an analyzer grating used to resolve the interference pattern, which is much smaller than the pixels in the detector. The absorption grating causes that only sections of the interference pattern pass through and get to the detector. [3, p.196]
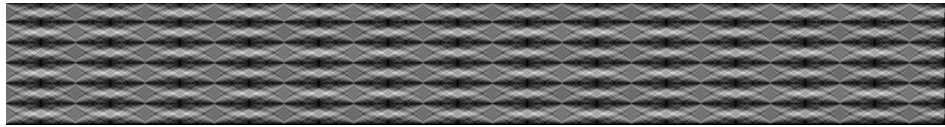
Figure 1.2: Simulated Talbot carpet: interference pattern behind grating G1 travelling from left to right. [3, p.196]

Moiré Fringes Grating alignment in a Talbot-Lau interferometer is required because of the Moiré-Fringes that can appear. If one of the three gratings is misaligned compared to the others, fringes appear in the acquired images. The misalignment can stem from a shift in the z direction in figure 1.1 or a tilting of the grating in the xy-plane. These Moiré-Fringes, as can be seen in figure 1.3, cause irregularities in the image and therefore want to be avoided.
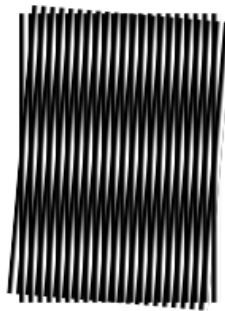

Figure 1.3: A moiré pattern, formed by two sets of parallel lines, one set inclined at an angle of 5° to the other. [9]

Phase-stepping Phase stepping is the concept of moving one absorption grating (G0 or G2) perpendicular to the beam direction (in x direction in figure 1.1). This enables to calculate to three quantities attenuation, differential phase and dark-field from the signal the detector receives.

Flat-field correction The fixed-pattern noise which can for example stem from inhomogeneity in the beam can influence image quality or in case of computed tomography can lead to artefacts. To avoid this flat-field correction can be used. Flat-field correction only works on noise which is the same in each image. For flat-field correction it is necessary to acquire an image without the sample in the field of view. This flat-field image can then be used to normalize the acquired image of the sample. The fixed-pattern
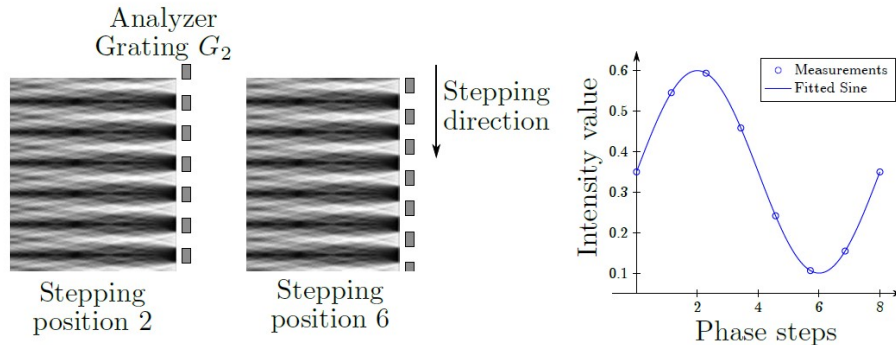
Figure 1.4: Left: phase stepping. The Talbot carpet is sampled at different positions of grating G2. Right: the intensities at different stepping positions form the sinusoidal phase stepping curve. From this curve, attenuation, differential phase and dark-field can be calculated. [3, p.198]

noise is largely reduced in the flat-field corrected image. [4]

Tomography   The previous paragraphs explained the principle of 2D imaging. But to gain all the information possible it is useful to obtain images from multiple angles of the sample so that a 3D image can be reconstructed. This can be done by rotation the sample. The acquired images can then be reconstructed into a three dimensional image.

1.4   Procedure

The procedure of the thesis consists of familiarising with the existing setup, the existing code used to control this setup and the piezo-motor. After the mounting of the new piezo, the implementation included establishing connectivity with the motor and altering the script in such a way that all existing functions were still working. Furthermore, new functions were written for the continuous motion of the G0.

The alignment of the Talbot-Lau interferometer was achieved by moving and tilting G2, with the screws on the mounting, until the grating structure was aligned vertical to the Talbot carpet. Different source gratings were interchanged and compared by taking a phase-stepping measurement and calculating the mean visibility. The grating with the largest visibility was then used as G0.

After implementing the piezo into the system, the focus was on the comparison of discrete phase stepping and continuous movement of G0 during image acquisition. The flat-field corrected images of a sample acquired with both procedures were then compared.

Chapter 2

Setup

The Talbot-Lau interferometer setup used for this thesis can be seen in figure 2.1. On the left in the figure 2.1 is the x-ray source located (shown in red). The three gratings are shown in purple. The piezo-motor, to move G0, is indicated with yellow. Marked in green is the sample, which sits on a vertical and a rotation motor. On the right of the figure, shown in blue, is the detector.
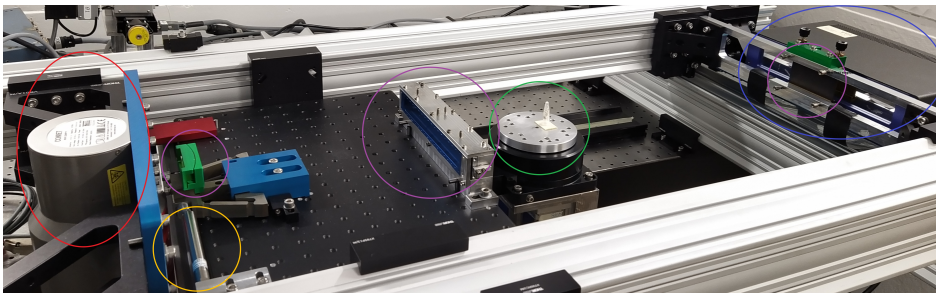

Figure 2.1: Setup of the Talbot-Lau interferometer at PSI

X-ray source   The x-ray source used in the setup is a Comet MXR-225HP/11. The tube consists of a high power tungsten anode, a directional beam and dual focal spot. [1]
The x-ray tube is operated at 70kV, 10mA and 0.4 FOC, in this thesis.

Gratings   The Talbot-Lau interferometer setup consists of three gratings: an absorption grating (G0) to create an array of partial self-coherent sources, a π-shifting phase grating (G1) which produces the Talbot-carpet downstream and a second absorption analyzer grating (G2). Two of them (G0 and G1) are fixed in a solid fixture to the table. They cannot be moved (except for
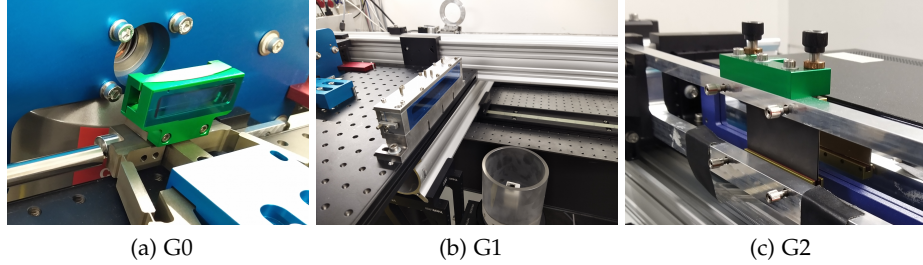
(a) G0   (b) G1   (c) G2

Figure 2.2: Fixtures of the gratings

G0, which can be moved perpendicular to the beam direction for phase-stepping) or tilted, as can be seen in figures 2.2 (a) and (b). This is to simplify the alignment process. Because they are fixed to the table, they do not need to be aligned manually.

G2, on the other hand, is mounted magnetically to six screws as seen in 2.2 (c). These screws change the position of G2 in all three spatial dimensions and are used to align the gratings.

The gratings are of the following type (see also table 2.1):

- G0: gold on graphite

- G1: silicon for π-shift at 46keV etched

- G2: gold on graphite

	G0	G1	G2
period [μm]	4.8	6.47	9.92
gold height [μm]	150	9.20	150
duty cycle	0.5	0.5	0.5
dimension (L x W) [mm x mm]	45 x 10	80 x 17	80 x 40

Table 2.1: Specifics of the gratings used in the setup

Because G2 does not cover the whole detector area (as can be seen in figure 2.2 (c)), the acquired image cannot be used entirely.

Piezo The motor used to move G0 is a P-841.60 Piezo-motor and the motor is controlled by a E-709 Piezo controller (for more information see [7]), which is connected with USB to a PC.

The maximum length of movement of the motor is 90 μm. [8] The movement can either be absolute to a defined position or according to a wavetable.

The wavetable can be freely designed, most interesting for this thesis are the three general shapes shown in figure 2.3. Six different wavetables can be defined. The wavetables, which were used in this thesis are shown in table 2.3. These wavetables can be called by a function by their numbers; for example moving the Piezo motor with wavetable 5 means a linear movement with amplitude 4.5μm.

To control the piezo from a python function, the modules **GCSDevice** and **pitools** from the **pipython** library are used.
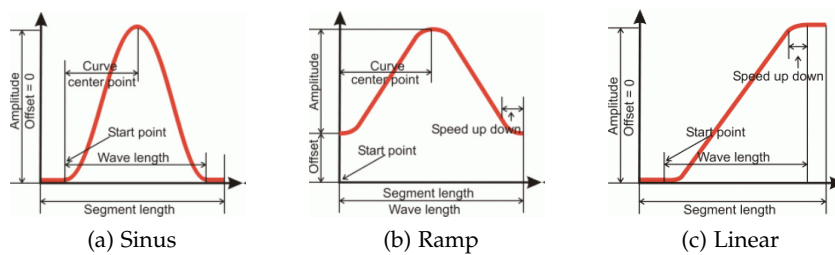

Figure 2.3: Possible movement patterns of piezo wavetables [6, p.99-101]

	movement	amplitude [μm]	number of wavetable points
1	linear	80	2000
2	ramp	44	1200
3	linear	20	2000
4	linear	4.4	2000
5	linear	4.5	2000
6	ramp	88	2400

Table 2.2: Wavetables

Sample   In this setup, the sample is positioned between G1 and G2. The sample is mounted on a vertically moving and a rotating motor. The vertical motor enables to take flat field images without having to remove the sample manually. It is also useful for larger samples to take measurements on multiple vertical positions, so that the entire height of the sample is imaged. The rotating of the sample enables tomography.

Detector   To detect the signal, a Dectris Titlis T02402_75-0 detector is used in the setup. This detector uses cadmium telluride crystals to convert the x-ray signal.

Chapter 3

Grating alignment

It is important in the Talbot-Lau interferometer setup to align the three gratings. If this is neglected, the resulting Moiré-fringes will cause irregularities in the acquired images.

Alignment Before the alignment, the intensity image without a sample in the beam can be seen in figure 3.2 (a). The Moiré-Fringes are clearly visible with five periods in the vertical component.
The number of periods in the vertical component can be reduced by tilting the grating with the two screws on top of the fixture. After tilting the grating the right amount; this is done by gradually moving and checking the image; the vertical component vanishes. This can be seen in figure 3.2 (b).
There is however still a horizontal component of the Moiré-Fringes visible. There are approximately 4 periods visible, this is a result of the distance between the gratings that have not been adjusted yet. After adjusting the distance on grating G2 (by turning all the four screws in the front of the mount the same amount) the absorption image shows only one fringe in the vertical direction that can not be fully removed. This concludes the alignment.
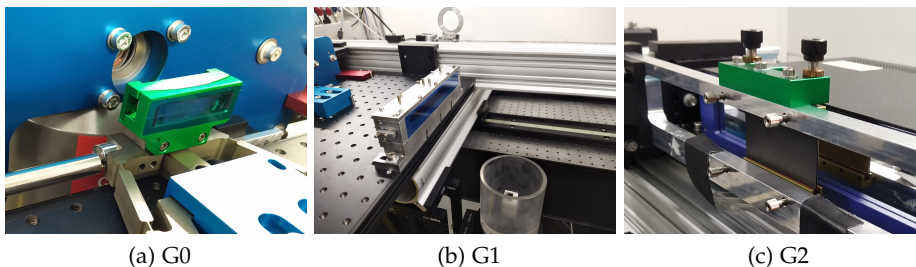

(a) G0   (b) G1   (c) G2

Figure 3.1: Fixtures of the gratings

11

(a) Before alignment

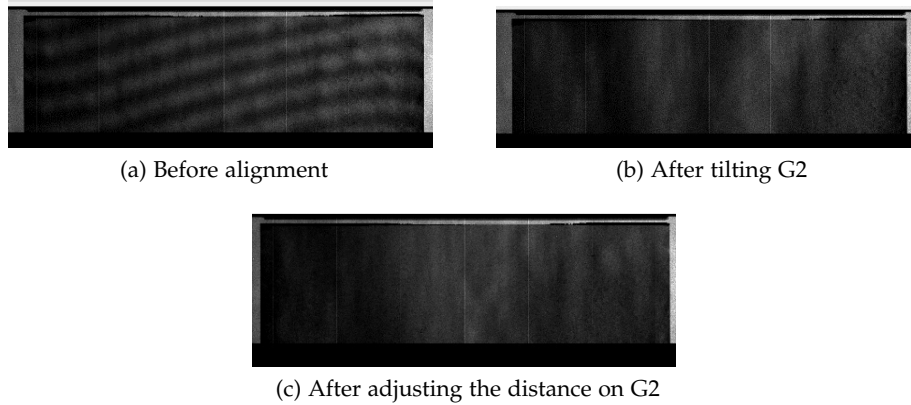(b) After tilting G2

(c) After adjusting the distance on G2

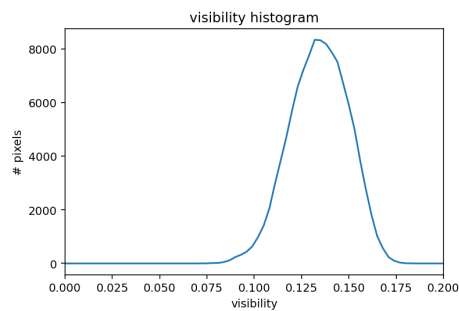Figure 3.2: Absorption image of different stages of grating alignment

Figure 3.3: Visibility of a phase-stepping scan in grating region

Visibility After the grating alignment, a phase-stepping scan was performed to check the visibility. For this measurement a different detector (XCounter XC-Thor) was used. A mean visibility of 13.57% in the grating region was achieved, as evident in the visibility histogram from figure 3.3.

Chapter 4

G0 testing

To achieve the best visibility possible, multiple G0 gratings were tested under the same conditions and the obtained images compared according to the visibility. All the tested gratings are gold plated graphite gratings, etched at PSI, with a period of 4.8μm, as discussed in section 2.

Testing conditions   Each of the gratings was inserted into the mount where it got bent slightly to account for the conical beam geometry of the setup. The mounting consists of two parts which are fitted together. The grating was placed on one part. The second part was carefully fitted on the first part with the grating. This pressed the grating in the designed curved shape. The mount with the grating inside was secured with six screws. The visibility with the inserted grating was checked by performing a phase-stepping scan without a sample. From this image, the visibility was determent and compared to the other tested gratings.

Comparison   The visibility histogram of all the four tested grating can be found in figure 4.3 and the mean visibility for the grating region can be found in table 4.1.

Figure 4.1: G0 with mount

	Visibility mean value [in %]
Grating 1	12.78
Grating 2	13.67
Grating 3	14.55
Grating 4	13.27

Table 4.1: Mean visibility in grating region in a phase-stepping scan
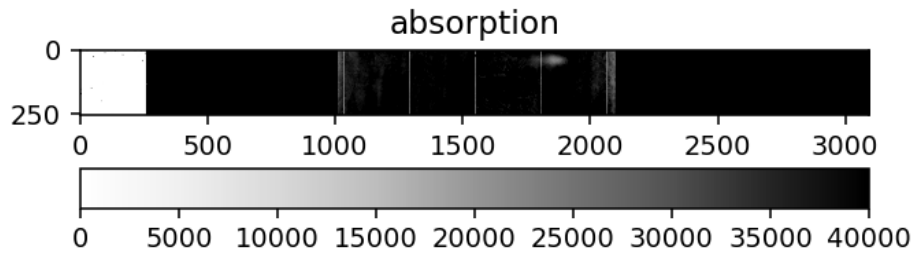

Figure 4.2: Absorption image of phase stepping measurement

As can be seen from the table 4.1 the gratings differ up to 1.77% in visibility. These values are with taking into account, that the periods of the different grating are not exactly the same, which is determined by signal retrieval. To adjust the precision of the fit for grating three and four, the period of the phase-stepping motion had to be adjusted such that the phase-stepping movement is over one period as precisely as possible.

From the data in table 4.1 grating three was chosen with the highest mean visibility of 14.55%. Therefore grating three is used from here on for all further measurements.

When doing a measurement there is a light spot with nearly zero absorption. This can be seen in figure 4.2 in the top right corner of the grating area. This spot stems from the chosen G0 grating.
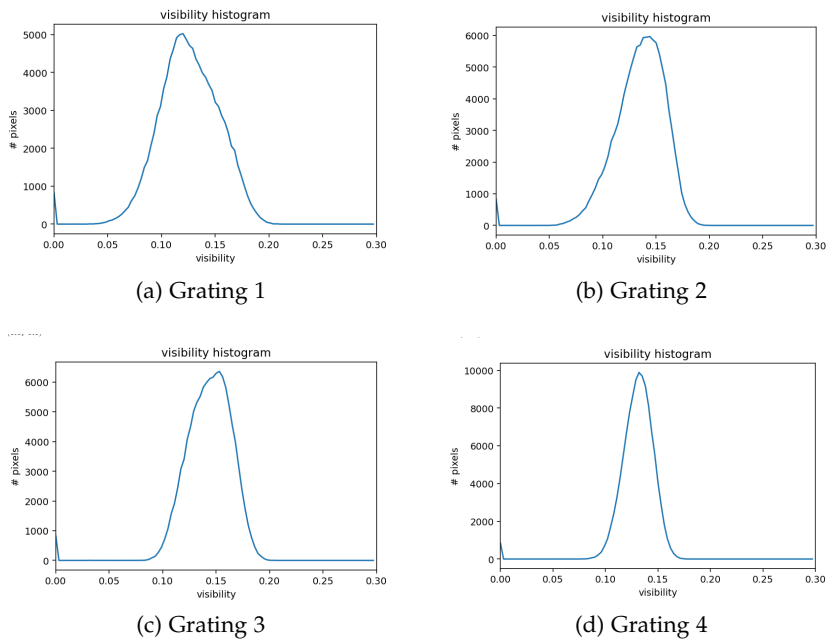
(a) Grating 1

(b) Grating 2

(c) Grating 3

(d) Grating 4

Figure 4.3: Visibility histograms of the different tested G1 gratings, achieved by phase-stepping measurements

Chapter 5

Projection imaging

For the phase-stepping of G0, a function was implemented that acquired and saved the data. A parameter can be handed to the function that specifies the mode of the piezo operation. The first mode uses the piezo for phase-stepping where it does not move during image acquisition (see section 5.1). The second mode is used to acquire images with a continuously moving G0 grating (see section 5.2).

5.1 Phase-stepping

Parameters   If the function is called for phase-stepping, the period has to be given. The period means the total movement length of the G0 grating. Most of the time the movement should equal to one period of the grating (for this setup, the period is approximately 4.4μm). Furthermore, the exposure time for each image (meaning the exposure time per phase-step) has to be given as well as how many phase-steps are made in the entire scan.

Procedure   First of all the x-ray source is initialised. This is done manually with the external voltage source. Then the script initialises the detector and the piezo motor. The imaging process consists of alternating between taking an image and moving the G0 grating one phase-step. The grating is stationary during the image acquisition and only moves in between images. Once all the phase-steps are completed the motor moves G0 back to the starting position and the acquired images are saved to the predefined location.

5.2 Continuous movement

Parameters   If the function is called for continuous movement of G0, the shape of the movement has to be specified (see section 2). As in the phase-

stepping case the exposure time for each image and how many images are take in the entire scan need to be given.

For the continuous equivalent to the phase-stepping movement a linear motion was chosen as it uses the same area of G0 and is closest to discrete phase stepping for comparison reasons. Therefore in this thesis, the function is always called with wavetable four which is a linear movement over one period which equals 4.4μm (see section 2.1).

Procedure   To be able to move the piezo continuous simultaneously to the acquisition the python package **threading** was used. With the threading implemented the two subfunctions which control the acquisition and the movement of the piezo can then run simultaneously. It is important to achieve the correct timing of moving the grating G0 at the same time as the acquisition is in progress or else there could be a loss of needed data. Once the acquisition is finished and the piezo is moved back to the starting position, the data is saved and the measurement finished.

5.3 Vertical projection image

With the previously defined phase-stepping or continuously moving G0 vertical projection imaging can now be undertaken.

Procedure   Since the vertical projection is implemented with flat-field-correction the function starts with moving the sample vertically to zero (which means moving the sample to the lowest possible position, out of the field of view) to take the first flat image. The flat-field image is taken by calling the phase-stepping function. After that, the motor moves the sample to the highest position which is defined when calling the vertical projection image function. Then another phase-stepping image is taken. The number of vertical steps as well as the vertical distance the motor moves the sample between images is defined when calling the function. For each of the vertical steps the phase-stepping function is called. After finishing the acquisition the sample is moved down by the predefined distance. After all the images with the sample have been acquired, the vertical motor moves the sample to zero again, and the last flat-field image is taken.

5.4 Comparison discrete and continuous movement

To compare the continuous movement of G0 and the discrete phase-stepping vertical projection images were taken. Both movements are taken under the same conditions and without moving the sample in between.

Measurement   The vertical projection function is used for the comparison measurement. The movement of G0 spans over 4.4μm for both the discrete phase-stepping movement (in five steps) and the linear movement. The duration of one exposure is set to 2.0s and the vertical movement is done in five steps of size 8mm for both acquisitions. The sample used for the images is a small tube with murine lungs which can be found in figure 5.1.

Figure 5.1: Sample: Murine lungs

Comparison   In figures 5.2, 5.3 and 5.4 the result of the vertical projection function is displayed grouped by absorption, phase and dark field. To obtain these images, the image shift was calculated and the mean of the overlaying region of the two vertical neighbouring images was taken.
The continuous motion scans G0 uniformly instead of step-wise and therefore depends differently on the G0 structure but the image quality does not differ very much. To obtain better image quality the scan needs to be done over multiple periods.

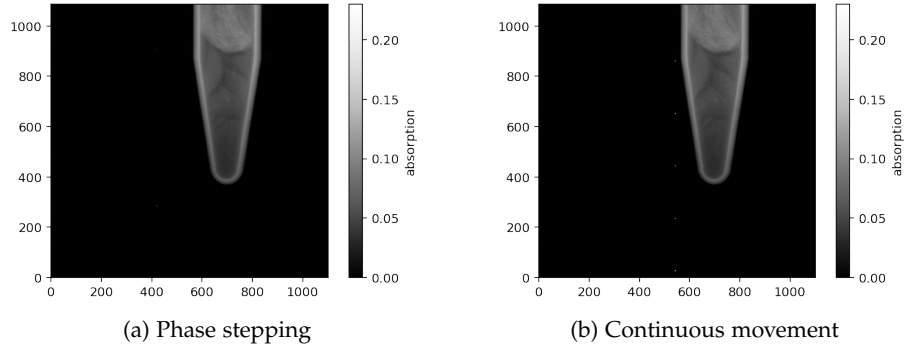(a) Phase stepping   (b) Continuous movement

Figure 5.2: Absorption of vertical projection image with discrete or continuous movement of G0

(a) Phase stepping   (b) Continuous movement
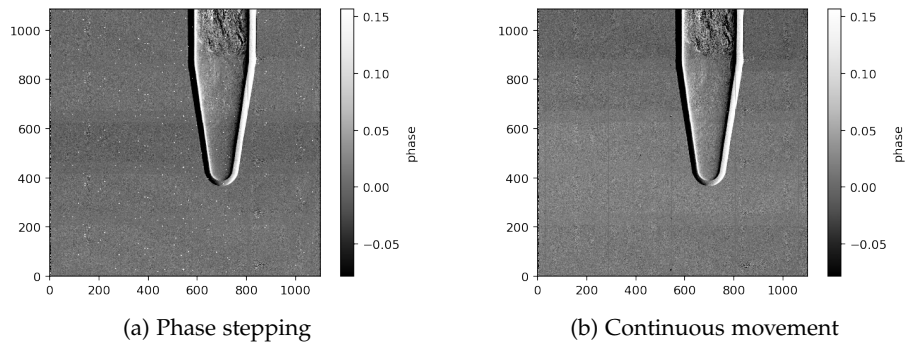
Figure 5.3: Phase of vertical projection image with discrete or continuous movement of G0

(a) Phase stepping   (b) Continuous movement
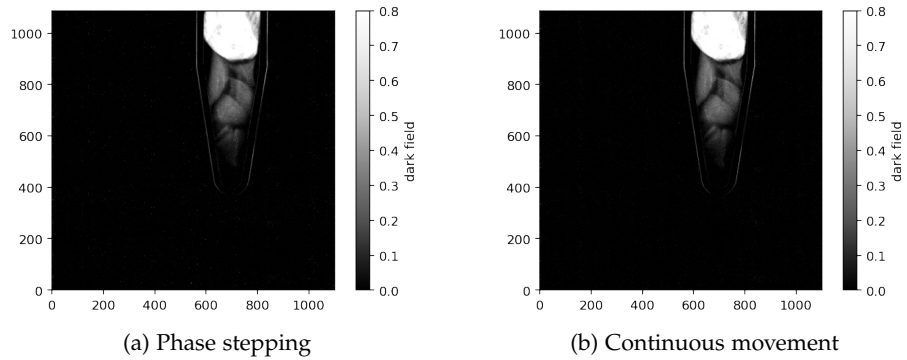
Figure 5.4: Dark field of vertical projection image with discrete or continuous movement of G0

Chapter 6

Computed tomography

Computed tomography is x-ray imaging of a sample from multiple angles. This is achieved by rotating the sample. With the acquired images it is possible to reconstruct a three dimensional image of the sample.

To implement the tomography a function is defined. Just like for the projection imaging (see section 5.1), there is a parameter which defines if the movement of G0 is continuous or discrete. For the continuous movement see section 6.2 and for the phase-stepping see section 6.1.

Parameters   Other important parameter which have to be defined are the highest point the vertical motor moves the sample to during the tomography, the number of vertical steps that are done in the tomography and the minimal vertical range the sample moves during the tomography also need to be specified. If the minimal vertical range is a negative value the movement of the sample starts at the defined highest point and moves further down. If this value is positive the movement starts at the defined position and the sample is moved further up.
Additionally, because the function implements flat-field correction the vertical position the sample is moved to, for taking the flat image also needs to be given. This means that for every tomography scan (which means for every vertical position) one image with the sample and two flat images are available.

6.1   Phase stepping

When the G0 grating is moved in steps the total distance which G0 travels during the phase-stepping and the number of phase-steps need to be specified just as in section 5.1 for the phase-stepping.

Procedure When the tomography function is called upon at first, the vertical positions are defined by accounting for the movement direction. Then for every vertical position another function is called. In this function at the beginning one flat image gets taken. This means the sample is moved to the defined flat position, where it is not in the field of view and then the phase-stepping function is called. After acquiring the flat-field image a tomography scan is taken for every phase-step. After G0 has been moved for the phase-stepping the detector starts the measurement for the tomography a few images earlier than the rotational motor starts to rotate the sample. This is to ensure that no rotational angle is missing. Once the whole rotation and the whole acquisition are finished, the motor rotates back to the starting point and the images are saved. Then the piezo motor moves G0 one phase-step further and the next tomography is acquired. After all the phase-steps are done, there is a second flat image taken, again by moving the sample vertically out of the field of view and then taking a phase-stepping measurement.

6.2 Continuous movement

When the G0 grating is moved continuously the wavetable used for the movement pattern needs to be specified.

Wavetable For the continuous movement to capture all the data it is necessary to have each phase position for each angle. This means there has to be a shift such that this condition is satisfied either by an offset in space (see figure 6.1 (a)) after each rotation or an offset in time (see figure 6.1 (b)). The option to implement an offset in time is used here because it is easier to achieve. An example of this principle can be seen in figure 6.2. This example is for five different phase-positions and a wavetable with a ramp shape (see figure 2.3 (b)). The image of the first angle of the second rotation is not taken in the first G0 position but in the second. Therefore a shift occurs and all the data is available without altering the motion pattern.
For the following images the wavetable two (see table 2.1) was used. This wavetable has a ramp shape, an amplitude of 44μm and 2400 wavetable points.

Procedure When the tomography function is called the beginning is the same as in the phase-stepping case (see section 6.1). Firstly, the vertical positions are defined and then for every vertical position another function is called where at the beginning one flat image is taken. After acquiring the flat-field image the piezo, the detector and the rotational motor are initialised and the right values (given by the input parameters) are set. After that the acquisition and the continuous piezo movement are started simultaneously,

(a) Offset in space
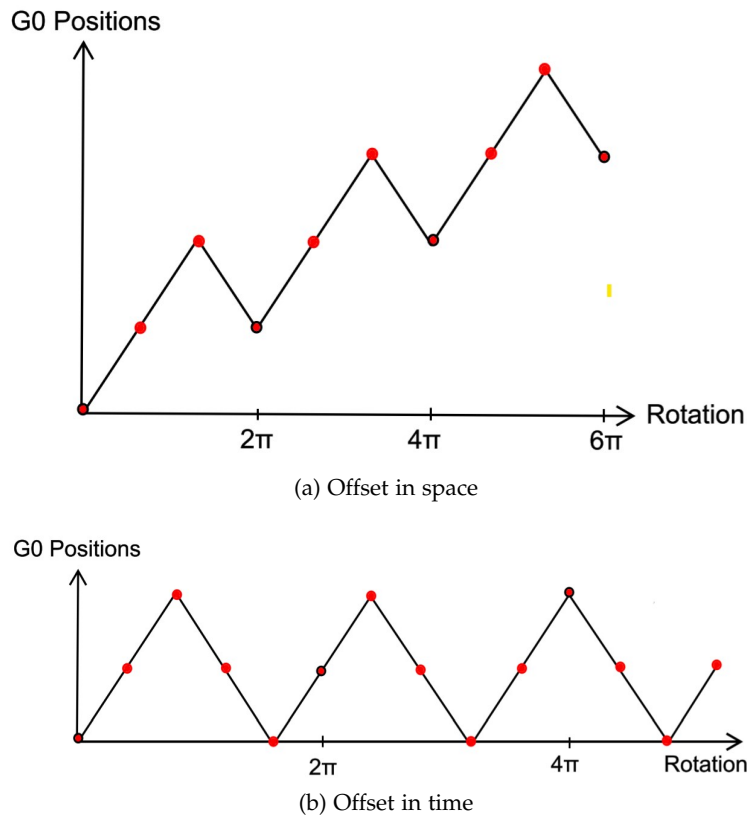

(b) Offset in time

Figure 6.1: Two phase-stepping offset options

via threading. The rotation of the sample is initiated a few images later. This ensures that all the angles of the rotating sample are captured and no data is missing. Once the rotation of the sample, the movement of G0 and the acquisition are finished, the rotational motor rotates the sample back to the initial position and the data is saved. After that the second flat image is taken.

Result   To retrieve the signal from the acquired data, phase tagging is necessary. Phase-tagging enables signal retrieval even if the phase-stepping positions are not uniformly distributed (as can be seen in figure 6.2). In this case, the phase-tagging did not work because the accuracy of the period was not sufficient. In the phase image of the tomography scan very strong artefacts are visible even though the image is already flat field corrected. The artefacts could originate from imprecise signal retrieval because of the used movement pattern or imprecise movement of the piezo motor. The latter is very unlikely because of the motors high precision.
Period accuracy is very important in the used implementation of tomogra-
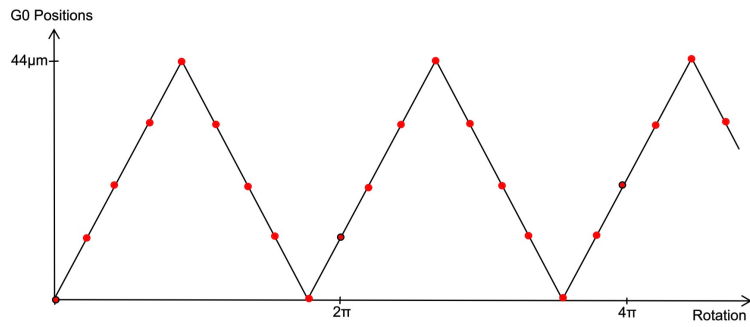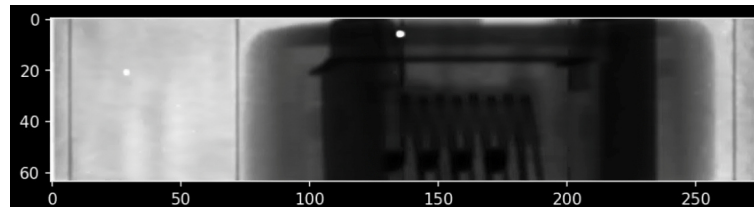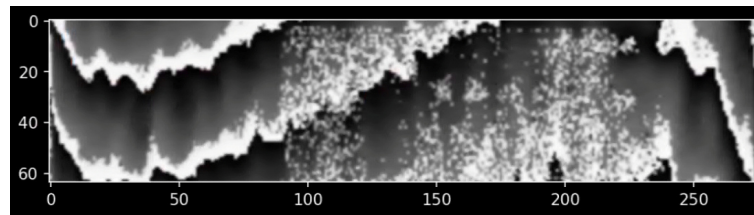
Figure 6.2

(a) Absorption

(b) Phase

Figure 6.3: Tomography scan of an Ethernet connector with continuous movement of G0

phy. This is because if the period is wrong by a small offset, this offset is added again with each rotation. So after five rotations the difference is five times the offset. If there would have been more time as a solution to this problem one phase-step-shift per rotation could have been implemented. This is not as dependent on the accuracy of the period because the error cannot stack for each rotation.

Chapter 7

Outlook

Projection image   The next step in improving the projection images could be to compare different movement patterns for G0 and investigate, if a certain pattern improves the image quality.

Tomography   The next step in the progress of the tomography would be to go back to easier motion patterns and go from there to more and more sophisticated motions. Different movement patterns of G0 could be analyzed against each other, to determine if there is a difference in image quality.
To lower the dose of x-rays delivered to the sample and to speed up the image acquiring process, a sliding window phase-stepping could be implemented (as described in [10]).

Bibliography

[1] COMET AG, Herrengasse 10, 3175 Flamatt, Switzerland. *MXR-225HP/11 Product Description*, 04 2018. Available at https://www.comet-xray.com/CometXRay/media/Content/pdf_mxr-225hp_11_en_v1.pdf, version 7.

[2] Matias Kagias, Zhentian Wang, Vitaliy A Guzenko, Christian David, Marco Stampanoni, and Konstantins Jefimovs. Fabrication of au gratings by seedless electroplating for x-ray grating interferometry. *Materials Science in Semiconductor Processing*, 92:73–79, 2019.

[3] Andreas Maier, Stefan Steidl, Vincent Christlein, and Joachim Hornegger. *Medical Imaging System, An Introductory Guide*. Springer Open, 2018.

[4] Vincent Van Nieuwenhove, Jan De Beenhouwer, Francesco De Carlo, Lucia Mancini, Federica Marone, and Jan Sijbers. Dynamic intensity normalization using eigen flat fields in x-ray imaging. *Opt. Express*, 23(21):27975–27989, Oct 2015.

[5] Franz Pfeiffer, Martin Bech, Oliver Bunk, Philipp Kraft, Eric F Eikenberry, Ch Brönnimann, Christian Grünzweig, and Christian David. Hard-x-ray dark-field imaging using a grating interferometer. *Nature materials*, 7(2):134–137, 2008.

[6] Physik Instrumente (PI) GmbH & Co. KG, Auf der Roemerstrasse 1, 76228 Karlsruhe, Germany. *PZ222E User Manual E-709 Digital Piezo Controller, 1 Channel, -30 to 130 V*, 01 2019. Available at https://www.physikinstrumente.com/fileadmin/user_upload/physik_instrumente/files/Compact_Downloads_for_Software_CD/E-709.Digital-Piezo-Controller.zip, version 1.2.0.

[7] Physik Instrumente (PI) GmbH & Co. KG, Auf der Roemerstrasse 1, 76228 Karlsruhe, Germany. *E-709 Compact and*

Cost-Optimized Digital Piezo Controller, 10 2020. Available at https://static.physikinstrumente.com/fileadmin/user_upload/physik_instrumente/files/datasheets/E-709-Datasheet.pdf.

[8] Physik Instrumente (PI) GmbH & Co. KG, Auf der Roemerstrasse 1, 76228 Karlsruhe, Germany. *P-841 Preloaded Piezo Actuators*, 04 2020. Available at https://static.physikinstrumente.com/fileadmin/user_upload/physik_instrumente/files/datasheets/P-841-Datasheet.pdf.

[9] Wikipedia, the free encyclopedia. *Moiré pattern*, 04 2007. [Online; accessed May 26, 2021], Available at https://en.wikipedia.org/w/index.php?title=Moir%C3%A9_pattern&oldid=1015456762.

[10] I Zanette, M Bech, A Rack, G Le Duc, P Tafforeau, C David, J Mohr, F Pfeiffer, and T Weitkamp. Trimodal low-dose x-ray tomography. *Proceedings of the National Academy of Sciences*, 109(26):10199–10204, 2012.